*IOSR Journal of Applied Physics (IOSR-JAP)*
*e-ISSN: 2278-4861.Volume 13, Issue 5 Ser. III (Sep. – Oct. 2021), PP 34-46*
*www.iosrjournals.org*

# Phonon dynamical behaviour of Cesium & Thallium halides along with Ammonium-$d_4$ chloride ($ND_4Cl$)

Shukla, S. K[1], Mishra, K. K[2]; Kanaujia Kushagra[3]
[1]*Department of Applied science & Humanities, Goel Institute of Tech.& Management, Lucknow*
[2]*Associate Director-Accreditation and Quality assurance cell, Chitkara University, Chandigarh*
[3]*St. Francis College, Lucknow*

***Abstract :*** *To study the lattice dynamics of Cesium halides (CsCl at 78K & 298K, CsBr, CsI), Thallium halides TlCl, TlBr) as well Ammonium-$d_4$ chloride ($ND_4Cl$) under phonon dynamical properties, a new phenomenological model, van der Waals force shell model (VTSM) incorporating with van der Waal interactions (vWI) along with long-range screened Coulomb and three body interactions (TBI) in the framework of rigid shell model for short-range interactions, effective up to the second neighbour in these halides, has been evolved by us. We have seen that incorporation of van der Waals interaction enabled us producing a vast study of lattice dynamical as phonon dynamical properties & other derivable properties of Cesium Chloride structure solid with the use of 14 parameters. Through this model phonon dynamical properties are in good agreement with available experimental data with the help of theory and experimental results.*

***Keywords --*** *Lattice dynamics, Phonon dispersion curves, Combined density of states.*

Date of Submission: 15-10-2021 Date of Acceptance: 30-10-2021

## I. Introduction:

The study of thermal properties of monovalent heavier metal halides as CsCl crystal solids (CsCl at 78 K, CsCl at 298 K, CsBr, CsI, TlCl, TlBr & Ammonium-$d_4$ chloride ($ND_4Cl$) with application of various physical conditions and using several techniques, both theoretically and experimentally, have received considerable interest in recent years. The survey of the phonon dynamical behaviour of these halides on elastic constants [6,7,8,9] and Debye temperature variations [1-3,4,5] and their interpretations by means of theoretical models [1-3 & 10-18] with moderate success, has motivated the present author to the basic need for a lattice dynamical model for the satisfactory description of their interesting thermal properties. Kellermann [10] (BvK lattice theory) the first using rigid ion model (RIM) by considering the ions of the crystal to be rigid, undeformable and unpolarizable spherical particles, was failed to interpret the dynamical, optical and elastic properties of these crystals. After that in progress of lattice dynamics, deformation dipole model (DDM) of Karo and Hardy [11] rigid shell model (RSM) of Dick and Overhauser [13] and Woods et al.[14] were formulated by two different groups of workers. As the DDM allows only the redistribution of charges in deformed electron cloud while the shell model considers the relative displacement. So both effects (deformation and displacement) are present in ionic crystals. A general way to remove this deficiency is to include the deformation of electron shells in the framework of RSM. The most prominent amongst them are breathing shell model (BSM) of Schroder [15], the deformable shell model [DSM] of Basu and Sengupta [16] and three-body force shell model (TSM) of Verma and Singh [1-3]. Further, Singh and coworkers.[1-3] used extended three-body-force shell model (ETSM) which is an amalgamation of RSM and DDM. ETSM contains **(i)** the two-body long-range coulomb interaction and short-range repulsion effective up to second neighbour ions (i) the long-range three body forces and (ii) the dipole character of constituent atoms. Despite of these successes ETSM has revealed some features which do not have much physical significance. In our earlier papers [39-45] we have investigated the phonon dynamical behaviour of CsCl structure solids at various temperature with the application of our most realistic model, van der Waals three body force shell model (VTSM) for the lattice dynamics of various CsCl-structured crystals introducing the effect of van der Waals interactions (VWI) and three body interactions (TBI) in the framework of RSM, where the short-range interactions have been considered up to the second neighbours by us.

Furthermore, here in this paper, we are extending our study for the crystals such as CsCl at 78K & 298K, CsBr, CsI, TlCl at 100K, TlBr at 80K along with Ammonium-$d_4$ chloride ($ND_4Cl$) at 85K of the same group (CsCl structured solids) to check the applicability to produce complete lattice dynamics and other derivable properties of CsCl crystals by application of various physical parameters with the help of our new developed model van der Waals Three body force shell model (VTSM).

## II. Theory and Method of Computation:

Inclusion of the effects of van der Waals interactions and three-body interactions in the frame work of both ions Polarizable rigid shell model (RSM), the general formalism of present model (VTSM) can be derived from the crystal potential whose relevant expression per unit cell is given by

$$\Phi(r) = \Phi_{LR}(r) + \Phi_{SR}(r) \quad (1)$$

where the first term $\Phi_{LR}(r)$ ($\Phi$ ) represents the long-range Coulomb and three body interaction (TBI) energies expressed by

$$\Phi_{LR}(r) = \sum_{ij} \frac{Z_i Z_j e^2}{r_{ij}} \{1 + \sum_{ijk} f(r_{ik})\} = \frac{\alpha_M Z^2 e^2}{r} \left\{1 + \frac{16}{Z} f(r)\right\} \quad (2)$$

where Z is the ionic charge parameter of $i^{th}$ ion, $r_{ij}$ separation between $i^{th}$ and $j^{th}$ ion, f ($r_{ik}$) is the three body force parameter dependent on nearest-neighbour separation $r_{ik}$ and is a measure of ion size difference [19] and $\alpha_M$ is Madelung constant ( –1.762670). The second term in (1) is short-range energy contributions from overlap repulsion and van der Waals interactions (vdWI) expressed as [18, 26]

$$\Phi_{SR}(r) = Nb \sum_{i,j=1}^{2} \beta_{ij} exp\left[\frac{r_i + r_j + r_{ij}}{\rho}\right] + \sum_{ij} \frac{C_{ij}}{r_{ij}^6} + \sum_{ij} \frac{d_{ij}}{r_{ij}^8} \quad (3)$$

where the first term is the Hafemeister and Flygare (HF) potential [29]. The second term and third term represent the energy due to vdW dipole-dipole (d-d) and dipole-quadrupole (d-q) interactions, respectively. By using the crystal energy expression given in equation (1), the equations of motion of two cores and two shells can be written as:

$$\omega^2 MU = (R + Zm\ C'\ Zm)\ U + (T + Zm\ C'\ Ym)\ W \quad (4)$$

$$O = (T^T + Ym\ C'\ Zm)\ U + (S + K + Ym\ C'\ Ym)\ W \quad (5)$$

Here M, Zm and Ym are diagonal matrices representing the ion masses, the ion charges and the shell charges respectively. The short-range interactions of type core-core, core-shell and shell-shell are given by the matrices R, T and (S + K = $\zeta$ reducing number of adjustable parameters through *Cowley et.al.*) respectively, while *C'* specifies the long-range Coulomb interactions. U and W are polarization vectors where U specifying ionic displacements and W along with $Y_m$ the dipole moments of the ions. The elements of matrix Zm consists of the parameter Zm thereby giving the modified ionic charge.

$$Zm = \zeta = \pm Z \sqrt{1 + (12/Z) f_0} \quad (6)$$

The elimination of W from eqns. (6) and (7) leads to the secular determinant

$$|D(\vec{q}) - \omega^2 MI| = 0 \quad (7)$$

For the frequency determination. Here D (q) is the (6×6) dynamical matrix given by

$$D(q^{\rightarrow}) = (R' + Zm\ C'\ Zm) + (T + Zm\ C'\ Ym) \times (S + K + Ym\ C'\ Ym)\text{-}1\ (TT + Ym\ C'\ Zm) \quad (8)$$

The numbers of adjustable parameters have been largely reduced by considering all the short-range interactions to act only through the shells.

The expressions derived for elastic constants from eqn. (7) corresponding to VTSM are obtained as

$$C_{11} = \frac{e^2}{4a^4}\left[0.7010Z_m^2 + \frac{A_{12}+2B_{12}}{6} + \frac{A_{11}+B_{22}}{4} + 5.4283\zeta^2\right] \quad (9)$$

$$C_{12} = \frac{e^2}{4a^4}\left[-0.6898Z_m^2 + \frac{A_{12}-4B_{12}}{6} - \frac{B_{11}+B_{22}}{4} + 5.4283\zeta^2\right] \quad (10)$$

$$C_{44} = \frac{e^2}{4a^4}\left[-0.3505Z_m^2 + \frac{A_{12}+2B_{12}}{6} + \frac{B_{11}+B_{22}}{4}\right] \quad (11)$$

In view of the equilibrium condition $\left[\left(\frac{d\Phi}{dr}\right)_0 = 0\right]$ we obtain

$$B_{11} + 2B_{12} + B_{22} = -0.6780Z_m^2 \quad (12)$$

Where $Z_m^2 = Z^2\left[1 + \frac{16}{Z} f_0\right]$ (13)

$f'(0) = \left(\frac{df}{dr}\right)_{r=r_0}$, $r_0 = a\sqrt{3}$ is the inter atomic separation.

The term $f_0$ is a function dependent on the overlap integrals of the electron wave functions and the subscript zero indicates the equilibrium value.

By solving the secular eqn. (7) along [q 0 0] direction and subjecting the short and long-range coupling coefficients to the long-wavelength limit $\vec{q} \rightarrow 0$ , two distinct optical vibration frequencies are obtained as

$$(\mu\omega_L^2)_{q=0} = R_0' + \frac{(Z'e)^2}{\nu f_L} \cdot \frac{8\pi}{3}\left(1 + 12Z_m^{-2}\, Zr_0 f_0'\right) \quad (14)$$

$$(\mu\omega_T^2)_{q=0} = R_0' + \frac{(Z'e)^2}{\nu f_T} \cdot \frac{4\pi}{3} \quad (15)$$

where the abbreviations stand for

$$R_0' = R_0 - e^2\left[\frac{d_1^2}{\alpha_1} + \frac{d_2^2}{\alpha_2}\right]:$$

$$Z' = Z_m + d_1 + d_2 \quad (16)$$

$$f_L = 1 + \frac{8\pi\alpha}{3v}\left(1 + 12\, Z_m^2 Z r_0 f_0^{/}\right) \quad (17)$$

$$f_T = 1 - \frac{4\pi\alpha}{3v} \quad (18)$$

and $\alpha = \alpha_1 + \alpha_2$ (19)

Thus by using basic model parameters which have been determined by making use of the expressions for the three second order elastic constants ($C_{11}$, $C_{12}$, $C_{44}$), on the line of our previous paper **32-35** and the equilibrium condition, with inclusion of van der Waals interactions (VWI), the values of the input data (s) and model parameters of CsCl at 78K & 298K, CsBr, CsI, TlCl at 100K, TlBr at 80K along with Ammonium-$d_4$ chloride ($ND_4Cl$) at 85K have been listed in table 1, 2, 3, 4, 5, 6 & 7. The values of $A_{11}$, $A_{12}$, $A_{22}$, $B_{11}$, $B_{12}$, $B_{22}$, $C_{11}$, $C_{12}$, $C_{44}$ thus calculated from the knowledge of the values of various order of derivatives of ($r_0$) like $f/r_0$, $f^{/}r_0$, $f''r_0$, $f'''r_0$ are also obtained by using functional form ($r_0$)= $f_0 e^{-\frac{r}{\rho}}$. Further, these twelve (12) model parameters and vdW coefficients calculated through *SKV Approach as suggested by Singh and Singh*, have been used to compute [$b$, $\rho$, $f(r_0)$, $r_0 f^{/}(r_0)$, $A_{11}$, $A_{12}$, $A_{22}$, $B_{11}$, $B_{12}$, $B_{22}$, $d_1$, $d_2$, $Y_1$ & $Y_2$] of the VTSM with knowledge of experimental values of the equilibrium inter-atomic separation ($r_0$), the vibration frequencies $\nu_{LO}(\Gamma), \nu_{TO}(\Gamma)$, $\nu_{LO}(R), \nu_{LA}(R)$, $\nu_{TO}(X)$, $\nu_{TA}(X)$ and $\alpha_1, \alpha_2, \varepsilon\infty$ for these halides. The model parameters of VTSM have been used to compute the phonon spectra for these Cesium halides (CsCl structured solids as as CsCl at 78K & 298K, CsBr, CsI, TlCl, TlBr, $ND_4Cl$) for the allowed 56 non-equivalent wave vectors in the first Brillion zone at Computer Centre, B. H. U, Varanasi. The frequencies along the symmetry directions have been plotted against the wave vector to obtain the phonon dispersion curves (PDCs) from present used model. These curves have been compared with those measured by means of the coherent inelastic neutron scattering technique. Since the neutron scattering experiments provide us only very little data for the symmetry directions, we have studied the combined density of states (CDS) for the complete description of the frequencies for the Brillion zone.

The complete phonon spectra have been used to calculate the combined density of states (CDS), N ($v_j + v_j^{/}$) corresponding to the sum modes ($v_j + v_j^{/}$), following the procedure of Smart et al [34]. A histogram between N ($v_j + v_j^{/}$) and ($v_j + v_j^{/}$) has been plotted and smoothed out to obtain the CDS curves. These curves show well defined peaks which correspond to two-phonon Raman scattering peaks. Since no observed data on two-phonon IR/Raman spectra are available, these CDS peaks have been compared with the assignments calculated by using our present theoretical data and neutron data. Furthermore, the division of the Brillion zone in the present case is somewhat coarse; therefore, the fine structure of the infra-red and Raman shifts may not be reproduced completely. In order to interpret them, the critical point analysis has been used following the method prescribed by Burstein et al [33]. Besides above properties, the third and fourth order elastic constants (TOEC and FOEC) and pressure derivatives of second order elastic constants (SOEC) have also been calculated using the VTSM. For the calculation of Debye characteristics temperature $\Theta_D$ at various temperatures the calculated values of $C_V$ at different temperature T are to be taken and corresponding values ($\Theta_D$/T) is determined.

## III. Results and Discussion:

The calculations of the Cesium halides (CsCl at 78K & 298K, CsBr, CsI) have been performed with our model VTSM having fourteen (14) model parameters [$b$, $\rho$, $f(r_0)$, $r_0 f^{/}(r_0)$, $A_{11}$, $A_{12}$, $A_{22}$, $B_{11}$, $B_{12}$, $B_{22}$, $d_1$, $d_2$, $Y_1$ & $Y_2$] calculated by using expressions (from equation 5-13) and presented along with input data in Table 1, 2, 3, 4. These model parameters have been used to compute the phonon dispersion curves of CsCl at 78K & 298 K, CsBr, CsI with available experimental data for CsCl (78K) Ahmad *et. al* [33], CsCl (298K) Ahmad *et. al* [22], CsBr (80K) Rolandson and Raunio [34] and CsI (298K) Bürher and Hälg [24] as well as theoretical data CsCl (at 78K) Ahmad *et. al* [22] · CsCl (at 298K) Gupta and Upadhyaya[2], CsBr (at 80K) Singh *et. al.*[1-3] and CsI (at 298K) Singh *et. al.*[1-3]. The phonon dispersion curves (PDCs) for all the Cesium halides at specifically mentioned temperatures are almost similar but there are certain specific features which deserve special mention. Three-body interactions have influenced both LO and TO branches much more than the acoustic branches (LA and TA) in these halides. Another striking feature of the present model is noteworthy from the excellent reproduction of almost all the acoustic branches. The agreement achieved from the present model is also excellent for the longitudinal acoustic (LA) branch along [$q,q,q$] direction.

This may be particularly because the zone centre vibration frequencies have been used as input data in the calculation of model parameters. A quantitative interpretation of the general features of PDCs are also obvious from the present model when it predicts the gap between the acoustical and optical branches similar to forbidden gap between the valence and the conduction band. The agreement between our computed phonon spectra and experimental data is excellent in Table 5−8 for CsCl at 78 K, CsCl at 298 K, CsBr at 80K and CsI at RT. Our model *VTSM* has successfully explained the phonon anomalies even along ($q$00) and ($qqq$) directions. From figure 1-4 it is clear that *VTSM*, improves result of SM used calculation of CsCl at 78 K by 3.97% along

TO(X), 3.07% along LA(X), 2.16% along TA (X), 0.26% along LO(R), 0.52% along TO(R) and 2.4 % along LA(R) and TA(R) and improve the results of TSM used for the calculation of CsCl at 298 K by 0.887% along L*O*(X), 6.9767% along *LA*(X), 9.022% along TA (X), 1.0781% along LO(R), 1.33% along TO(R) and 3.94% along TA(R). The deviation between theory and experimental due to *SM* is maximum 4.61 % along LO(X) while due VTSM the deviation is maximum 0% along LO(X). In view of overall success, it may be concluded that our model provides a good agreement between theory and experiment and is certainly better than those yielded by theoretical workers [2,9,10,12,14,15,16,28]. It is obvious from these tables that the frequencies at X, R and M points reported from present model VTSM are very much close to the experimental values [22]. Similarly, for other Cesium halides like CsBr at 80K & CsI at RT, the agreement between our computed phonon spectra and experimental data is again excellent.

Also regarding thallous halides ( TlCl at 100K & TlBr at 80K) it is evident from figure 5 and 6 that the phonon dispersion curves (PDCs) for the thallous halides are quite similar with Cesium halides as three-body interactions have influenced both optical branches (LO and TO) much more than the acoustic branches (LA and TA) in these halides. Also the most significant feature of the present model is noteworthy from the excellent reproduction of almost all the acoustic branches. The agreement achieved from the present model is also excellent for the longitudinal acoustic (LA) branch along [*qqq*] direction. A qualitative comparison amongst frequencies at X, M and R symmetry points of measured PDCs and those reported from present study has been collected for thallous chloride (TlCl) and thallous bromide (TlBr) in tables 9 and 10 respectively. In view of overall success, it may be concluded that our model provides a good agreement between theory and experiment [7, 19] and is certainly better than those yielded by theoretical workers [2]. It is obvious from these tables that the frequencies at X, R and M points reported from present model VTSM are very much close to the experimental values. It is clear from the table 9 for TlCl that the percentage deviation of VTSM from the experimental values along the X - point could not be reported due to non-availability of experimental values. Our results of frequencies may however be used, in future, by the experimental workers to obtain a comparison between our values with their experimental results. Similarly, from the table 10 for TlBr, the percentage deviation of VTSM from the experimental values has no deviation along the TA(X) branch whereas that along the LA(X) branch it is 4.2 % and the percentage variations of VTSM from the experimental values along LO(X) branch, is within 1%. This reveals that our model is very close to the measured phonon dispersion curves (PDCs) of TlCl and TlBr along X- point. Also from the table 9, it is evident that along M – point, in case of TlCl the percentage deviation of VTSM from the experimental values is within 3.0% for all the branches, the maximum being 2.83% along TO (M) branch and no deviation along both acoustic branches LA(M) and TA(M). Similarly, in case of TlBr along M- point the percentage deviation of VTSM from the experimental values for all branches, has not been reported. Furthermore, it is clear from the table 10 for TlBr the percentage deviation of VTSM from the experimental values along R is also within 6.27 %, the maximum being 6.27 % for both optical branches LO(R) and TO(R) while for LA(R) and TA (R) it is 1.48 %. The percentage deviation of VTSM from the experimental values in case of TlCl along R – point could not be compared as no experimental data is available so far. However, we expect that our results of frequencies may be used in future by the experimental workers to obtain a correlation between our values with their experimental results.

Now in case of Ammonium-$d_4$ chloride ($ND_4Cl$) from table 11 and figure 7, it is quite evident that our model VTSM (with VWI & TBI effects) has improved results of MRIM [20] by 20% along LO(Γ), 2.66% along TO(Γ), 8.77% along LO(X), 20.44% along TO (X), 6.09% along LA(X), 12.11% along TA(X), 3.03% along LO(M), 3.03% along TO(M), 9.52% along LA(M), 28.33% along TA(M), 8.27% along LO(R), 8.27% along TO(R), 2.55% along LA(R) and 2.55% along TA(R) showing that the deviation between theoretical and experimental values due to MRIM [20] is maximum 28.33% along Ta(M) while due to our developed model VTSM, the deviation is found to be4 only 0.73% maximum along TO(X).

## IV. Conclusions:

The present paper shows a systematic investigation of the Lattice dynamics of Cesium Chloride structure solid comprising CsCl (at 78K & 298 K), CsBr at 80K, CsI at RT, TlCl at 100K, TlBr at 80K and & Ammonium-$d_4$ chloride ($ND_4Cl$). The VTSM model proposed for this purpose, has been developed by us incorporating the effects of van der Waals interactions (VWI) and three-body interactions (TBI) in the frame work of rigid shell model (RSM) originated by Cochran et. al [27, 30] It is evident that the overall fair agreement between our theoretical and experimental results established through the present model VTSM, is reasonably good for describing the phonon dispersion curves, Debye temperatures variations, combined density of states and two phonon infra-red and Raman spectra of ionic cesium chloride structure solid. The definite improvements achieved by VTSM in the framework of RSM over the models such as BSM, DSM & TSM, clearly shows that interaction mechanism beyond the dipolar approximation, is mainly due to van der Waals interaction which is better manifestation of many-body interaction comprising three-body interaction component. That is why, with the help of these qualities of VTSM over other models, the present VTSM model

may be understood to provide a powerful and simple approach for a comprehensive study of the harmonic as well as the other properties such as anharmonic properties (Cauchy discrepancy, TOEC, SOEC and their pressure derivatives etc) of the crystals under consideration. The only limitation of the model is the requirement of the knowledge of certain experimental information which has been used as input data.

**Acknowledgment**

The author with others are thankful to Prof. (Dr) Rishi Asthana, Director of GITM, Lucknow for providing the necessary facilities. One of us (S K Shukla) is also thankful to Dean Academics Prof. (Dr) Devendra Agarwal GITM, LKO (UP) for his consistent encouragement, and helping attitude. We are also thankful to Computer Centre, BHU, Varanasi, India for providing computational assistance. I sincerely thankful to our Chairman sir Er. Mahesh Agarwal who always stood by me like an inspirational force. At last we are grateful to our guide and mentor (Late) Prof. Dr K. S. Upadhyaya without his encouragement, constant cooperation and blessings.

**Table-1: Input data and Model parameters for CsCl at 78K & 298K**

$[C_{ij}]$ and B (in $10^{12}$ dyne/cm$^2$), ν (in THz), $r_0$(in$10^{-8}$cm), $\propto_1$ (in $10^{-24}$cm), b (in $10^{-12}$erg ), $\rho$ (in$10^{-8}$cm)

| Input Data | | | | | Model Parameters | | |
|---|---|---|---|---|---|---|---|
| Properties | CsCl at 78 K | | CsCl at 298 K | | Parameters | CsCl at 78 K | CsCl at 298 K |
| | Values | Ref. | Values | Ref. | | Values | Values |
| $C_{11}$ | 4.260 | [6] | 4.068 | [6] | b | 0.273 | 0.2490 |
| $C_{12}$ | 1.300 | [6] | 1.200 | [6] | $\rho$ | 0.378 | 0.3110 |
| $C_{44}$ | 1.092 | [6] | 1.100 | [6] | $f(r_0)$ | −3.98 | −3.2800 |
| B | 17.000 | [29] | 17.000 | [29] | $r_0 f'(r_0)$ | 21.5241 | 21.7418 |
| $r_0$ | 3.540 | [1] | 3.570 | [1] | $A_{12}$ | 6.5878 | 6.5844 |
| $\nu_{LO}(\Gamma)$ | 4.900* | [22] | 4.930* | [22] | $B_{12}$ | −0.3863 | −0.3829 |
| $\nu_{TO}(\Gamma)$ | 3.170 | [22] | 3.010 | [22] | $A_{11}$ | −0.7240 | −0.8275 |
| $\nu_{LO}(R)$ | 3.810 | [22] | 3.710 | [22] | $B_{11}$ | −0.0197 | −0.0038 |
| $\nu_{LA}(R)$ | 2.020 | [22] | 1.970 | [22] | $A_{22}$ | 1.4497 | 1.6651 |
| $\nu_{TO}(X)$ | 3.000 | [22] | 2.820 | [22] | $B_{22}$ | −0.9242 | −1.0753 |
| $\nu_{TA}(X)$ | 1.350 | [22] | 1.300 | [22] | $d_1$ | 0.2825 | 0.2975 |
| $\propto_1$ | 2.798 | [1] | 2.798 | [1] | $d_2$ | 0.3902 | 0.3820 |
| $\propto_2$ | 2.653 | [1] | 2.653 | [1] | $Y_1$ | −2.2482 | −2.0818 |
| $\epsilon_0$ | 6.680 | [1] | 6.950 | [1] | $Y_2$ | −1.5432 | −0.2642 |

*Extrapolated value

**Table-2: Input data and Model parameters for CsBr at 80K & CsI at 298K**

$[C_{ij}]$ and B (in $10^{12}$ dyne/cm$^2$), ν (in THz), $r_0$(in$10^{-8}$cm), $\propto_1$ (in $10^{-24}$cm), b (in $10^{-12}$erg ), $\rho$ (in$10^{-8}$cm)

| Input Data | | | | | Model Parameters | | |
|---|---|---|---|---|---|---|---|
| Properties | CsBr at 80 K | | CsI at 298 K | | Parameters | CsBr at 80 K | CsI at 298 K |
| | Values | Ref. | Values | Ref. | | Values | Values |
| $C_{11}$ | 3.349 | [6] | 2.430 | [6] | b | 0.1902 | 0.3720 |
| $C_{12}$ | 1.002 | [6] | 0.636 | [6] | $\rho$ | 0.3260 | 5.7600 |
| $C_{44}$ | 0.962 | [6] | 0.666 | [6] | $f(r_0)$ | −0.0019 | −0.2090 |
| B | 13.01 | [30] | 6.870 | [24] | $r_0 f'(r_0)$ | 0.020 | −0.0126 |
| $r_0$ | 3.270 | [30] | 3.955 | [24] | $A_{12}$ | 6.8541 | 20.6045 |
| $\nu_{LO}(\Gamma)$ | 3.470* | [14] | 2.690* | [24] | $B_{12}$ | −0.3676 | 12.3893 |
| $\nu_{TO}(\Gamma)$ | 1.483 | [14] | 1.918 | [24] | $A_{11}$ | 1.1321 | 9.1051 |
| $\nu_{LO}(R)$ | 2.437 | [14] | 1.815 | [24] | $B_{11}$ | −0.0492 | −0.5170 |
| $\nu_{LA}(R)$ | 1.863 | [14] | 1.751 | [24] | $A_{22}$ | 1.7737 | 2.9079 |
| $\nu_{TO}(X)$ | 1.927 | [14] | 1.214 | [24] | $B_{22}$ | −0.3175 | −2.7613 |
| $\nu_{TA}(X)$ | 1.345 | [14] | 1.256 | [24] | $d_1$ | 0.3189 | 0.3094 |
| $\propto_1$ | 3.033 | [158] | 3.131 | [1] | $d_2$ | 0.4187 | 0.5033 |
| $\propto_2$ | 3.994 | [158] | 6.191 | [1] | $Y_1$ | −0.0492 | −0.0492 |
| $\epsilon_0$ | 6.450 | [13] | 5.650 | [1] | $Y_2$ | −0.0492 | −0.0492 |

**Table-3: Input data and Model parameters for TlCl at 100K & TlBr at 80K**

$[C_{ij}]$ and B (in $10^{12}$ dyne/cm$^2$), ν (in THz), $r_0$(in$10^{-8}$cm), $\propto_1$ (in $10^{-24}$cm), b (in $10^{-12}$erg ), $\rho$ (in$10^{-8}$cm)

| Input Data | | | | | Model Parameters | | |
|---|---|---|---|---|---|---|---|
| Properties | TlCl at 100 K | | TlBr at 80 K | | Parameters | TlCl at 100 K | TlBr at 80 K |
| | Values | Ref. | Values | Ref. | | Values | Values |
| $C_{11}$ | 4.690 | [32] | 4.399 | [15] | b | 0.2930 | 0.2652 |
| $C_{12}$ | 1,740 | [32] | 1.660 | [15] | $\rho$ | 0.4120 | 0.3490 |
| $C_{44}$ | 1.080 | [32] | 1.079 | [15] | $f(r_0)$ | −0.0045 | −0.0027 |

| | | | | | | | |
|---|---|---|---|---|---|---|---|
| **B** | 23.8 | [30] | 22.470 | [30] | $r_0 f'(r_0)$ | 0.0240 | −0.0152 |
| $r_0$ | 3.185 | [30] | 3.419 | [30] | $A_{12}$ | 11.5050 | 11.4950 |
| $\nu_{LO}(\Gamma)$ | 5.070 | [7] | 1.390 | [19] | $B_{12}$ | −0.5654 | −0.5545 |
| $\nu_{TO}(\Gamma)$ | 2.080 | [7] | 3.270 | [19] | $A_{11}$ | −0.4244 | −0.4234 |
| $\nu_{LO}(R)$ | 3.340 | [7] | 2.870 | # | $B_{11}$ | −2.2393 | −2.2403 |
| $\nu_{LA}(R)$ | 1.140 | [7] | 1.350 | [19] | $A_{22}$ | 2.7230 | 2.7091 |
| $\nu_{TO}(X)$ | 2.690 | [7] | 1.830 | [19] | $B_{22}$ | −2.4695 | −2.4687 |
| $\nu_{TA}(X)$ | 1.340 | [7] | 0.650 | [19] | $d_1$ | 0.8633 | 0.8593 |
| $\alpha_1$ | 4.800 | [31] | 5.100 | [31] | $d_2$ | 0.9726 | 0.9693 |
| $\alpha_2$ | 2.927 | [31] | 4.125 | [31] | $Y_1$ | −3.1014 | −3.1006 |
| $\epsilon_0$ | 37.600 | [6] | 32.500 | [15] | $Y_2$ | −0.2930 | −0.2652 |

# Calculated using LST (Lyddane–Sachs–Teller) relation

**Table-4: Input data and Model parameters for $ND_4Cl$**

$[C_{ij}]$ and B (in $10^{12}$ dyne/cm$^2$), ν (in THz), $r_0$(in$10^{-8}$cm), $\alpha_1$ (in $10^{-24}$cm), b (in $10^{-12}$erg ), $\rho$ (in$10^{-8}$cm)

| Input Data | | | Model Parameters | |
|---|---|---|---|---|
| **Properties** | **Values** | **Ref.** | **Parameters** | **Values** |
| $C_{11}$ | 4.69 | [8] | $Z_m$ | 0.8275 |
| $C_{12}$ | 1.57 | [8] | $r_0 f'(r_0)$ | 0.0119 |
| $C_{44}$ | 1.29 | [8] | $A_{12}$ | 5.9946 |
| **B** | --- | --- | $B_{12}$ | −0.3324 |
| $r_0$ | 3.3074 | [35] | $A_{11}$ | −0.9063 |
| $\nu_{LO}(\Gamma)$ | 7.7 | [35] | $B_{11}$ | −0.3998 |
| $\nu_{TO}(\Gamma)$ | 5.25 | [35] | $A_{22}$ | 2.9981 |
| $\nu_{LO}(R)$ | 5.32 | [35] | $B_{22}$ | −0.2040 |
| $\nu_{LA}(R)$ | 3.92 | [35] | $d_1$ | 0.2731 |
| $\nu_{TO}(X)$ | 4.07 | [35] | $d_2$ | 0.3872 |
| $\nu_{TA}(X)$ | 3.14 | [35] | $Y_1$ | −1.9240 |
| $\alpha_1$ | 2.0592 | [35] | $Y_2$ | −1.9421 |
| $\alpha_2$ | 2.9470 | [35] | | |

**Phonon Dispersion Curves of Monovalent heavier metal halides**

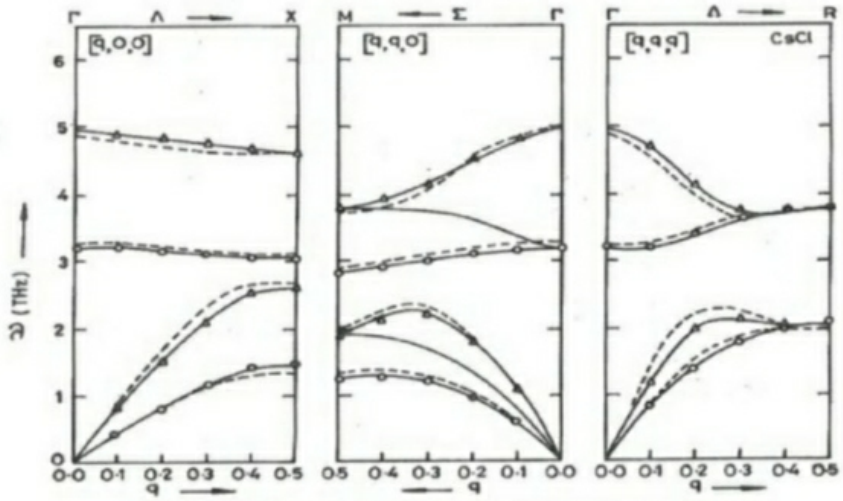


**Figure 1: Phonon Dispersion Curve for CsCl at 78 K**

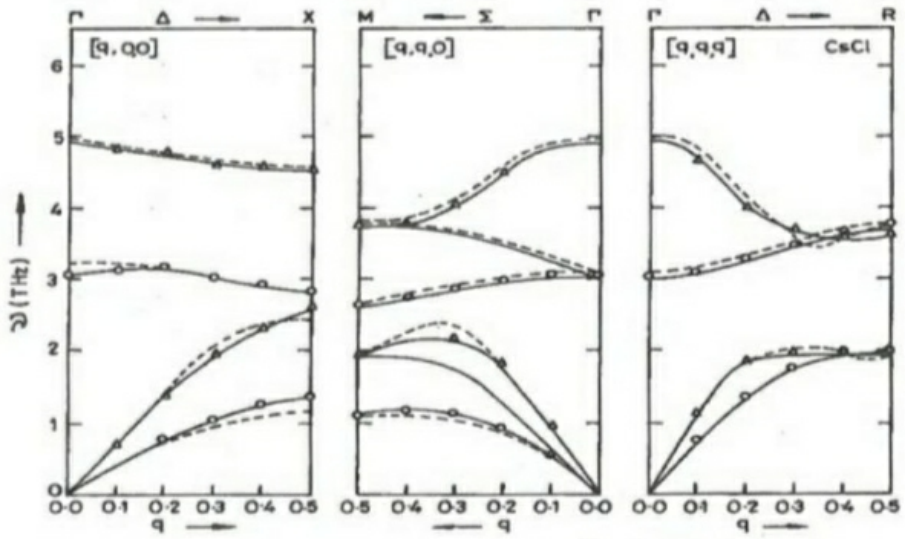


**Figure 2: Phonon Dispersion Curve for CsCl at 298 K**


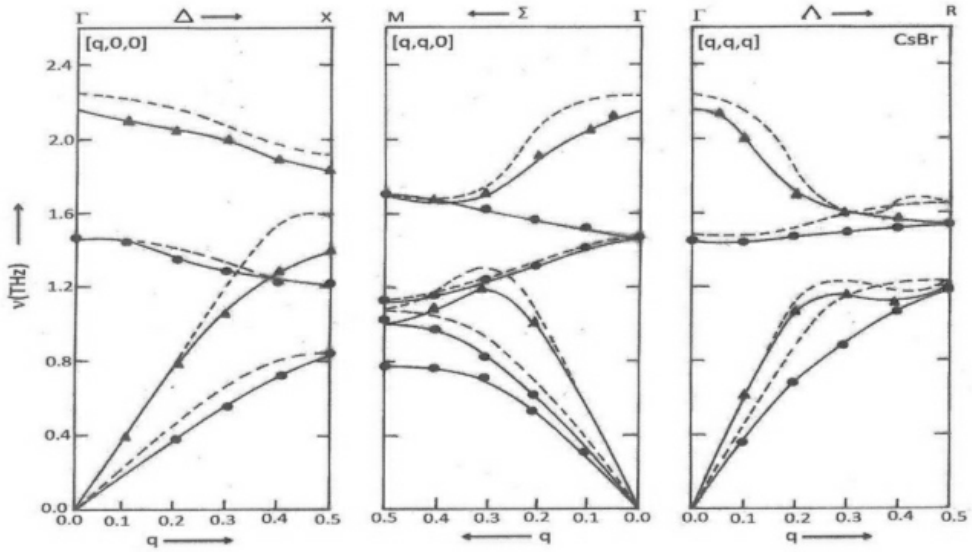


**Figure 3: Phonon Dispersion Curve for CsBr at 80 K**

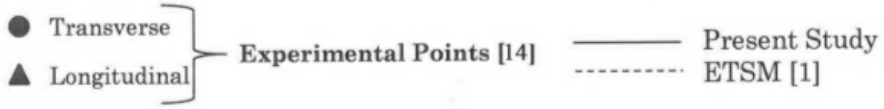

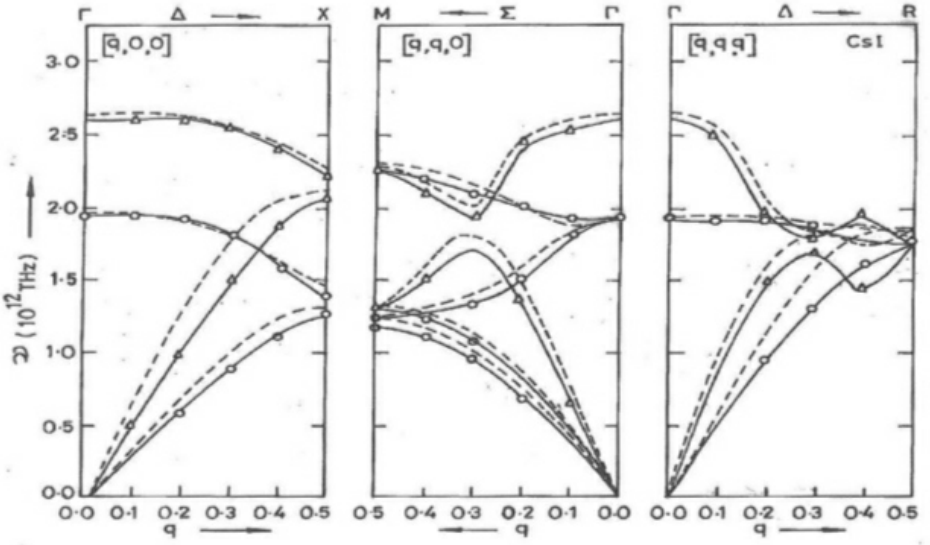


**Figure 4: Phonon Dispersion Curve for CsI**

● Transverse
▲ Longitudinal
**Experimental Points [24]**
——— Present Study
---------- ETSM [1]

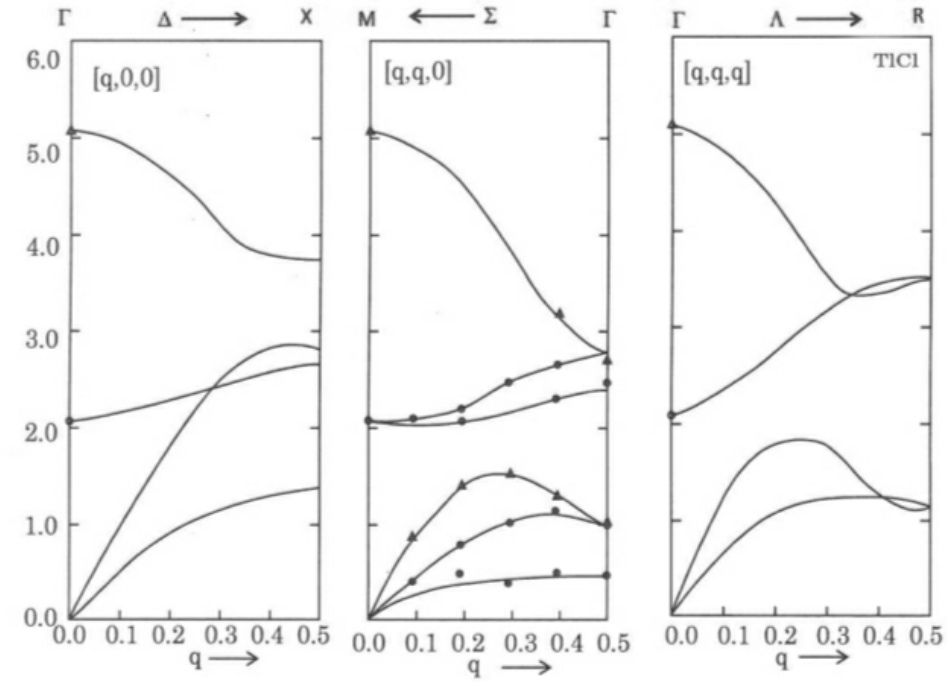


**Figure 5: Phonon Dispersion Curve for TlCl**

● Transverse
▲ Longitudinal
**Experimental Points [7]**
——— Present Study

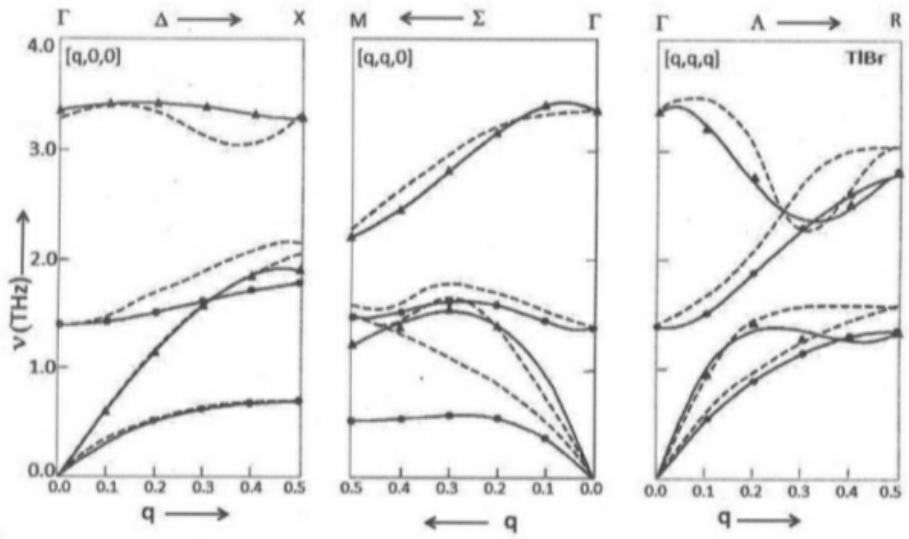


**Figure 6: Phonon Dispersion Curve for TlBr**


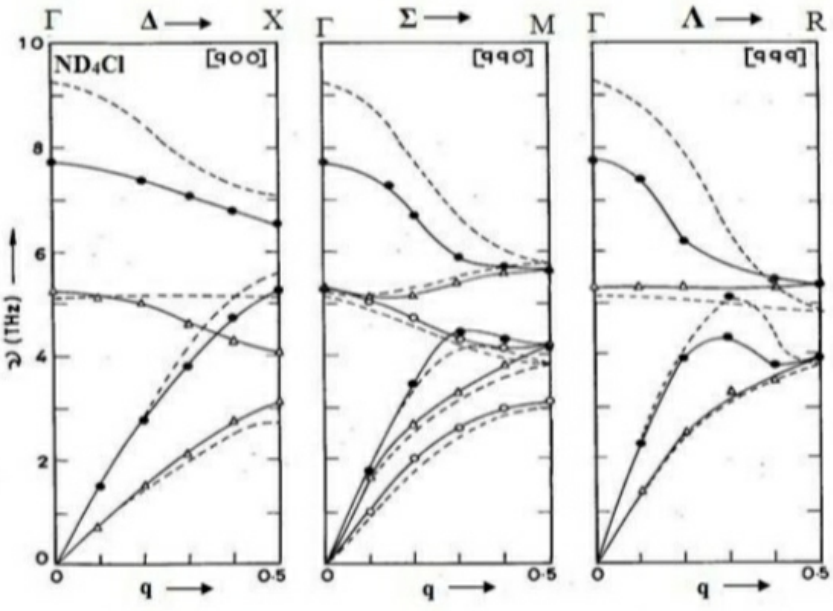


**Figure 7 Phonon dispersion curves for $ND_4Cl$ at 85K**

**Present Study**
**Teh & Brockhouse**
**Experimental Points**
**Longitudinal**
**Transverse**

**Table—5 Comparison of frequencies from various sources for CsCl (X and R points) at 78 K**

| Points | Branches | Exp [22] | SM [22] | | | VTSM (Present Study) | | | % Improvement (a−b) |
|---|---|---|---|---|---|---|---|---|---|
| | | | Value | ±Deviation | %Deviation (a) | Value | ±Deviation | %Deviation (b) | |
| X (0, 0, 0.5) | LO (THz) | 4.61 | 4.61 | 0 | 0 | 4.61 | 0 | 0 | 0 |
| | TO (THz) | 3.00 | 3.13 | −0.13 | 4.30 | 3.01 | −0.13 | 0.33 | 3.97 |
| | LA (THz) | 2.57 | 2.65 | −0.08 | 3.07 | 2.57 | 0 | 0 | 3.07 |
| | TA (THz) | 1.35 | 1.31 | 0.04 | 2.87 | 1.34 | 0.01 | 0.72 | 2.20 |
| R (0.5,0.5,0.5) | LO (THz) | 3.81 | 3.82 | −0.01 | 0.26 | 3.81 | 0 | 0 | 0.26 |
| | TO (THz) | 3.84 | 3.81 | 0.03 | 0.78 | 3.80 | 0.01 | 0.26 | 0.52 |
| | LA (THz) | 2.02 | 1.97 | 0.05 | 2.40 | 2.02 | 0 | 0 | 2.40 |
| | TA (THz) | 2.02 | 1.97 | 0.05 | 2.40 | 2.02 | 0 | 0 | 2.40 |

**Table—6 Comparison of frequencies from various sources for CsCl (X and R points) at 298 K**

| Points | Branches | Exp [22] | ETSM [2] | | | VTSM (Present Study) | | | % Improvement (a−b) |
|---|---|---|---|---|---|---|---|---|---|
| | | | Value | ±Deviation | %Deviation (a) | Value | ±Deviation | %Deviation (b) | |
| X (0, 0, 0.5) | LO (THz) | 4.51 | 4.55 | −0.04 | 0.90 | 4.51 | 0 | 0 | 0.89 |
| | TO (THz) | 2.82 | 2.79 | 0.03 | 0.03 | 2.82 | 0.03 | 1.05 | 0 |
| | LA (THz) | 2.55 | 2.37 | 0.18 | 7.00 | 2.55 | 0 | 0 | 6.98 |
| | TA (THz) | 1.30 | 1.18 | 0.12 | 9.00 | 1.30 | 0 | 0 | 9.00 |
| R (0.5,0.5,0.5) | LO (THz) | 3.71 | 3,75 | −0.04 | 1.08 | 3.71 | 0 | 0 | 1.08 |
| | TO (THz) | 3.71 | 3.76 | −0.05 | 1.40 | 3.71 | 0 | 0 | 1.40 |
| | LA (THz) | 1.97 | 1.98 | −0.01 | 0.49 | 1.98 | −0.01 | 0.49 | 0 |
| | TA (THz) | 1.97 | 1.98 | 0.08 | 4.00 | 1.97 | 0 | 0 | 4.00 |

**Table—7 Comparison of frequencies from various sources for CsBr (X and R points) at 80 K**

| Points | Branches | Exp [20] | ETSM [1] | | | VTSM (Present Study) | | | % Improvement (a−b) |
|---|---|---|---|---|---|---|---|---|---|
| | | | Value | ±Deviation | %Deviation (a) | Value | ±Deviation | %Deviation (b) | |
| X (0, 0, 0.5) | LO (THz) | 1.83 | 1.91 | −0.08 | 4.4 | 1.83 | 0 | 0 | 4.4 |
| | TO (THz) | 1.21 | 1.21 | 0 | 0 | 1.21 | 0 | 0 | 0 |
| | LA (THz) | 1.44 | 1.6 | −0.16 | 11.1 | 1.44 | 0 | 0 | 11.1 |
| | TA (THz) | 0.84 | 0.86 | −0.02 | 2.4 | 1.44 | 0 | 0 | 2.4 |
| R (0.5,0.5,0.5) | LO (THz) | 1.53 | 1.62 | −0.09 | 5.9 | 0.84 | 0 | 0 | 5.9 |
| | TO (THz) | 1.53 | 1.62 | −0.09 | 5.9 | 1.53 | 0 | 0 | 5.9 |
| | LA (THz) | 1.17 | 1.2 | −0.03 | 2.7 | 1.53 | 0.01 | 0.8 | 1.9 |
| | TA (THz) | 1.17 | 1.2 | −0.03 | 2.7 | 1.18 | 0.01 | 0.8 | 1.9 |

**Table—8 Comparison of frequencies from various sources for CsI (X and R points) at RT K**

| Points | Branches | Exp [24] | ETSM [1] | | | VTSM (Present Study) | | | % Improvement (a−b) |
|---|---|---|---|---|---|---|---|---|---|
| | | | Value | ±Deviation | %Deviation (a) | Value | ±Deviation | %Deviation (b) | |
| X (0, 0, 0.5) | LO (THz) | 1.36 | 1.40 | −0.04 | 2.94 | 1.38 | −0.02 | 1.47 | 1.5 |
| | TO (THz) | 0.82 | 0.86 | 0.04 | 4.87 | 0.83 | −0.01 | 1.22 | 3.6 |
| | LA (THz) | 1.30 | 1.33 | −0.13 | 2.30 | 1.30 | 0 | 0 | 2.3 |
| | TA (THz) | 0.79 | 0.82 | −0.03 | 3.79 | 0.80 | −0.01 | 1.26 | 2.5 |
| R (0.5,0.5,0.5) | LO (THz) | 1.10 | 1.13 | −0.09 | 2.73 | 1.13 | −0.03 | 2.73 | 2.7 |
| | TO (THz) | 1.11 | 1.11 | 0 | 0 | 1.11 | 0 | 0 | 0 |
| | LA (THz) | 1.11 | 1.11 | 0 | 0 | 1.11 | 0 | 0 | 0 |
| | TA (THz) | 1.10 | 1.13 | −0.03 | 2.73 | 1.10 | 0 | 0 | 2.3 |

**Table--9 Comparison of frequencies from various sources for TlCl (X and M points) at 80 K**

| Points | Branches | Exp [7] | ETSM [1] | | | VTSM (Present Study) | | | % Improvement (a−b) |
|---|---|---|---|---|---|---|---|---|---|
| | | | Value | ±Deviation | %Deviation (a) | Value | ±Deviation | %Deviation (b) | |
| X (0, 0, 0.5) | LO (THz) | --- | --- | --- | --- | 3.75 | --- | --- | --- |
| | TO (THz) | --- | --- | --- | --- | 2.70 | --- | --- | --- |
| | LA (THz) | --- | --- | --- | --- | 2.85 | --- | --- | --- |
| | TA (THz) | --- | --- | --- | --- | 1.40 | --- | --- | --- |

| | | | | | | | | | |
|---|---|---|---|---|---|---|---|---|---|
| **M** (0, 0.5,0.5) | LO (THz) | 2.73 | --- | --- | --- | 2.80 | 0.07 | 2.56 | --- |
| | TO (THz) | 2.47 | --- | --- | --- | 2.40 | 0.07 | 2.83 | --- |
| | LA (THz) | 1.04 | --- | --- | --- | 1.04 | 0 | 0 | --- |
| | TA (THz) | 0.52 | --- | --- | --- | 0.52 | 0 | 0 | --- |

**Table—10 Comparison of frequencies from various sources for TlBr (X and R points)**

| Points | Branches | Exp [19] | TSM [1] | | | VTSM (Present Study) | | | % Improvement (a−*b*) |
|---|---|---|---|---|---|---|---|---|---|
| | | | Value | ±Deviation | %Deviation (a) | Value | ±Deviation | %Deviation (b) | |
| **X** (0, 0, 0.5) | LO (THz) | 3.30 | 3.25 | 0.05 | 1.5 | 3.32 | 0.02 | 0.3 | 0.90 |
| | TO (THz) | 1.83 | 2.19 | −0.36 | 20.1 | 1.81 | 0.02 | 0.5 | 19.6 |
| | LA (THz) | 1.92 | 2.0 | 0.08 | 4.2 | 1.92 | 0 | 0 | 4.2 |
| | TA (THz) | 0.65 | 0.65 | 0 | 0 | 0.65 | 0 | 1.5 | 0 |
| **R** (0.5,0.5,0.5) | LO (THz) | 2.87 | 3.05 | −0.18 | 6.27 | 2.85 | 0 | 0 | 6.27 |
| | TO (THz) | 2.87 | 3.05 | −0.18 | 6.27 | 2.85 | 0 | 0 | 6.27 |
| | LA (THz) | 1.35 | 1.55 | −0.20 | 1.48 | 1.35 | 0 | 0 | 1.48 |
| | TA (THz) | 1.35 | 1.55 | −0.20 | 1.48 | 1.35 | 0 | 0 | 1.48 |

**Table—11 Comparison of frequencies from various sources for $ND_4Cl$ (X and R points) at 80 K**

| Points | Branches | Ref. [15] | MRIM [15] | | | VTSM (Present Study) | | |
|---|---|---|---|---|---|---|---|---|
| | | | Values | ± Deviation | % Deviation (a) | ± Deviation | % Deviation (b) | % Improvement (a−b) |
| Γ [0,0,0] | LO (THz) | 7.7 | 9.24 | 1.54 | 20 | ---- | ---- | 20 |
| | TO (THz) | 5.25 | 5.11 | 0.14 | 2.67 | ---- | ---- | 2.67 |
| **X** [0.5,0,0] | LO (THz) | 6.50 | 7.08 | 0.58 | 8.92 | 0.01 | 0.15 | 8.77 |
| | TO (THz) | 4.07 | 5.18 | 1.11 | 27.27 | 0.03 | 0.73 | 20.44 |
| | LA (THz) | 5.25 | 5.57 | 0.32 | 6.09 | ---- | ---- | 6.09 |
| | TA (THz) | 3.14 | 2.75 | 0.39 | 12.42 | 0.01 | 0.31 | 12.11 |
| **M** [0.5,0.5,0] | LO (THz) | 5.60 | 5.77 | 0.17 | 3.03 | ---- | ---- | 3.03 |
| | TO (THz) | 5.60 | 5.77 | 0.17 | 3.03 | ---- | ---- | 3.03 |
| | LA (THz) | 4.20 | 3.80 | 0.40 | 9.52 | ---- | ---- | 9.52 |
| | TA (THz) | 4.20 | 3.01 | 1.19 | 28.00 | ---- | ---- | 28.00 |
| **R** [0.5,0.5,0.5] | LO (THz) | 5.32 | 4.85 | 0.47 | 8.83 | 0.03 | 0.56 | 8.27 |
| | TO (THz) | 5.32 | 4.85 | 0.47 | 8.83 | 0.03 | 0.56 | 8.27 |
| | LA (THz) | 3.92 | 3.80 | 0.12 | 3.06 | 0.02 | 0.51 | 2.55 |
| | TA (THz) | 3.92 | 3.80 | 0.12 | 3.06 | 0.02 | 0.51 | 2.55 |

## References:


[1]. R. K. Singh, H. N. Gupta and M. K. Agrawal, Phys. Rev. B 17, 2, 894 (1978)
[2]. H.N. Gupta and R.S. Upadhyaya, Phys. Stat. Sol. (b) 102, 143 (1980).
[3]. Vipasha Mishra, S. P. Sanyal and R. K. Singh, Phil Mag. A 55, 5, 583 (1987)
[4]. M. Sorai, J. Phys. Soc. Japan 25, 421 (1968)
[5]. R.M. Redaumond and B. J.Yates, J. Phys. C5, 417 (1971)
[6]. R. P. Lowndes and D. H. Martin, Proc. R. Soc. Lond. A 308, 473 (1969).
[7]. Y. Fuzi; J. Phys. Soc. Japan, 44, 1237 (1978)
[8]. C. W. Garland and R. Renold, J. Chem. Phys 44 (1130) (1966)
[9]. J. F. Vetelino, S. S. Mitra, Phys. Rev. 178, 1349 (1969); Sol. Stat. Comm. 7, 1181 (1969)
[10]. E W Kellermann, Phill. Trans, Roy. Soc. (London) A238, 513 (1940); Proc Roy. Soc. A178, 17 (1941)
[11]. S. O. Lundqvist, Ark. Fys. 6, 25-38 (1952); 9, 435-36 (1955); 12, 263-7 (1957); 19, 113—21 (1961)
[12]. A.M Karo and J.R Hardy., J. Chem. Phys. 48, 3173 (1968).
[13]. B.G. Dick and A.W. Overhauser, Phys. Rev. 112, 90 (1958)
[14]. A.D.B. Woods, W. Cochran and B.N. Brockhouse, Phys. Rev. 119, 980 (1960).
[15]. U. Schroder, Solid Stat. Comm. 4, 347 (1966), ibid 88, 1049 (1993); A. N. Basu and S. Sengupta, Phys. Stat. Sol. **(b)** 29, 367--75 (1968)
[16]. M.P. Verma and R.K. Singh, Phys. Stat. Sol. 33, 769 (1969); 36, 335 (1969); 38, 851 (1970)
[17]. P. O. Lowdin, Ark. Mat. Astr. Fys. 35 A, 30 (1947)
[18]. E. R. Cowley and A. Okazaki, Proc. R. Soc. Lond. A 300, 45 (1965)
[19]. S. Rolandson and G. Raunio, Phys. J. Phys. Rev. C2, 1013 (1969), J. Phys. Rev. B4, 12, 4617 (1971),
[20]. G. E. Morse and A. W. Lawson, J. Phys. Chem. Solids, 26, 939 (1969),
[21]. A.A.Z. Ahemad, H. G. Smith, N. Wakabayashi and M. K. Wilkinson. Phys. Rev. B 6, 10, 3956 (1972).
[22]. W. Bührer and W. Hälg, Phys. Stat. Sol. (b) 46, 679 (1971).
[23]. C. Carabatos and B. Prevot, Canad. J. Phys. 50, 122 (1972)
[24]. P. O. Lowdin, Ark. Mat. Astr. Fys. 35 A, 30 (1947)
[25]. M. Born, Ann. Phys, 44, 605 (1914)
[26]. B. Szigeti, Trans. Farad. Roy. Soc. 45, 155 (1949); Proc. Roy. (London) A 204, 51 (1950)
[27]. Hafemeister D.W. and Flygare H.W. ,J. Chem. Phys. 43, 795 (1965).
[28]. W. Cochran, Proc, Roy. Soc. (Lond.) A 253, 260 (1959); Phys, Rev. Letter 2, 495 (1959); Phil, Mag. 4, 1082 (1959); Adv. Phys. 9, 387 (1960); Adv. Phys. 10, 401 (1961)

[29]. P. O. Lowdin, Ark. Mat. Astr. Fys. 35 A, 30 (1947)
[30]. S. O. Lundqvist, Ark. Fys. 6, 25-38 (1952); 9, 435-36 (1955); 12, 263-7 (1957); 19, 113—21 (1961)
[31]. H. H. Lal and Verma M.P., J. Phys. C 5, 543 (1972).
[32]. U. Kõhler, P. G. Johannson and W. B. J. Holzapfel, Phys. Condens. Matter 9, 5581 (1997)
[33]. Handbook of optical constants of solids, Ed E. D. D. Palik, V3, ISBN 0-12 544423-0, 721; 928 (1998)
[34]. R. Tessmann, A. H. Khan and W. Shockley, Phys. Rev. 92, 890 (1953); 161, 877 (1967)
[35]. S. Haussuhl; Phys. Rev. 165, 959 (1968)
[36]. E. Burstein, F. A. Johnson and R. Loudon, Phys. Rev. 144, 390 (1966)
[37]. C. Smart, G. R. Wilkinson, A. M. Karo and J. R. Hardy, Lattice Dynamics, edited by R.F.Wallis (Pergamon Press, Oxford, 1965)
[38]. H. C. Teh and B. N. Brockhouse, Phys. Rev. B3, 2733 (1971)
[39]. K.S Upadhyaya, Atul Pandey and Srivastava D.M., Chinese Journal of Phys., Vol. 44, 127 (2006).
[40]. K.K Mishra, G.K. Upadhyay and. K.S Upadhyaya, Phys. Rev. and Research Int. 2(2), 91-106, (2012)
[41]. K.K Mishra, K.S Upadhyaya., Int. Jour. of Sci. Engg. Res. 3 (8), 1-9, (2012)
[42]. K.K Mishra, K.S Upadhyaya, Physica Scripta (2012).
[43]. S.K.Shukla, K.K.Mishra, A.N.Pandey, G.K.Upadhyay, K.S.Upadhyaya, IOSR J. Appl. Phys. 2(4), pp 26-34 (2012).
[44]. S.K.Shukla, M.P. Srivastawa, K.K.Mishra, K.S.Upadhyaya, Asian J. Phys. Sci. 1(2) pp 84-104 (2012).
[45]. S.K.Shukla, K.K.Mishra, A.N. Pandey, G.K.Upadhyay, K.S.Upadhyaya, Int. J. Pure Appl. Phys. 9 (2), (pp 125-138) (2013)
[46]. S.K.Shukla, K.K.Mishra and K.S.Upadhyaya, Adv. Sci. Lett. (America) Vol 22, pp 3972-3977 (2016).
[47]. S.K.Shukla, K.K.Mishra, Journal of Advanced Physics Volume 6, Number 4 pp.465-624 (2017)
[48]. S.K.Shukla, K.K.Mishra and K.S.Upadhyaya, PINNACLE DES ACADEMIA Vol X, Issue X pp 22-27 (Jan, 2018)
[49]. S.K.Shukla, Law Kumar Pandey, K. S. Upadhyaya IOSR Journal of Applied Physics (IOSR-JAP) . Appl. Phys. 10(1), pp 01-11 (2018)

Shukla, S. K, et. al. "Phonon dynamical behaviour of Cesium & Thallium halides along with Ammonium-d4 chloride (ND4Cl)." *IOSR Journal of Applied Physics (IOSR-JAP)*, 13(5), 2021, pp. 34-46.